Electronic Supplementary Material (ESI) for Journal of Materials Chemistry A.

Supporting Information

Porous $NiMoO_{4-x}/MoO_2$ Hybrids as Highly Effective Electrocatalyst for Water Splitting Reaction

*Zhe Zhang[a], Xingxing Ma[a,b], and Jilin Tang[*a]*

[a] State Key Laboratory of Electroanalytical Chemistry, Changchun Institute of Applied Chemistry, Chinese Academy of Sciences, Changchun 130022, China

E-mail: jltang@ciac.ac.cn. Tel/Fax: (+86) 431−85262734

[b] University of Science and Technology of China, Hefei 230026, China

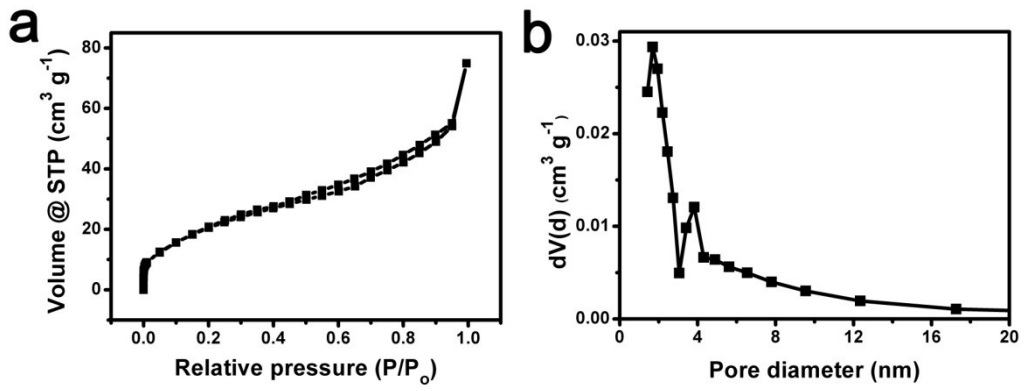

Figure S1. Nitrogen adsorption-desorptin isotherms (a) and pore size distribution curve (b) of $NiMoO_{4-x}/MoO_2$.

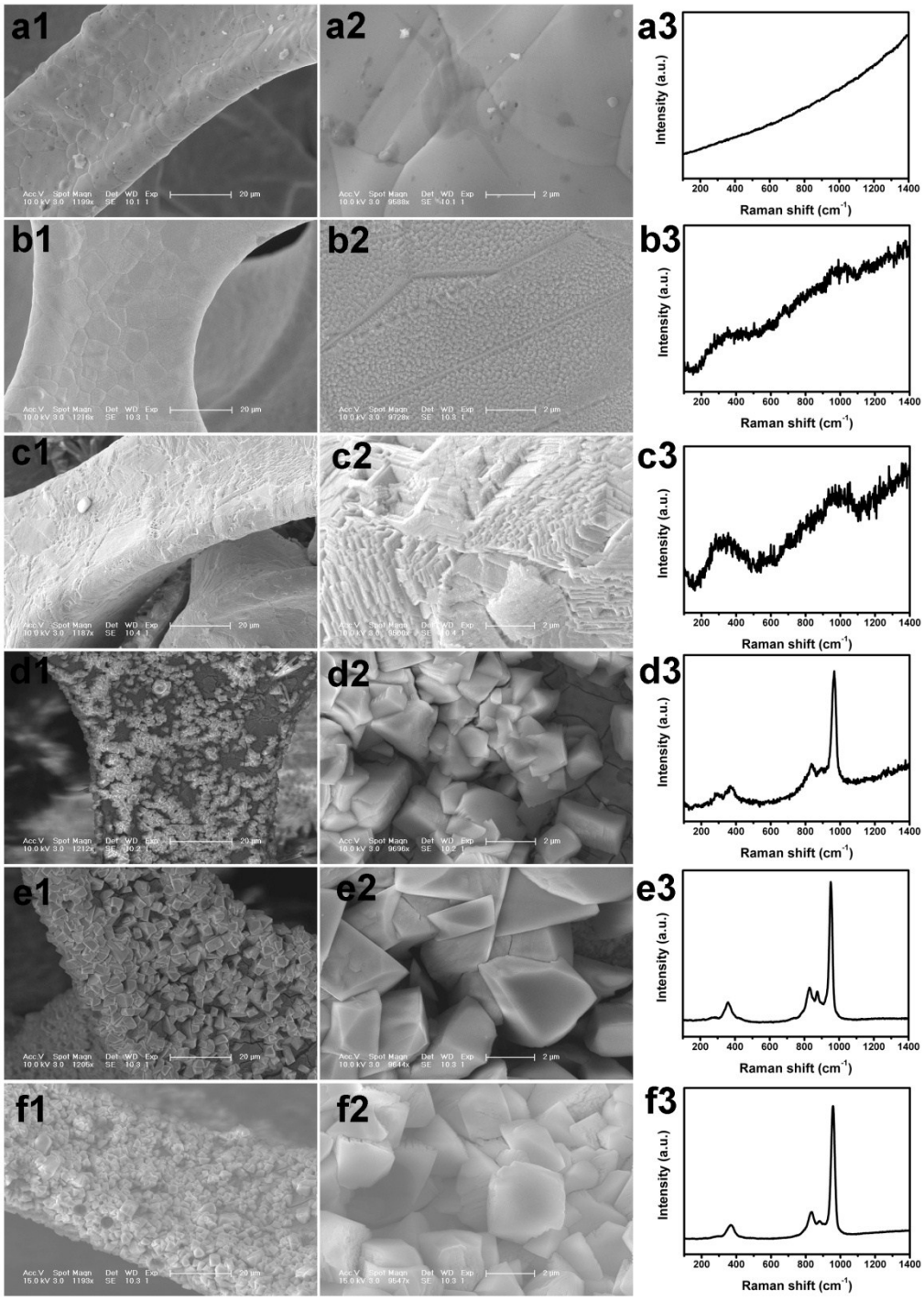

Figure S2. SEM images (**1** and **2**) with different magnification and corresponding Raman spectra (**3**) of the Precursor obtained after reaction for 0 h (a), 1 h (b), 2 h (c), 3 h (d), 4 h (e), and 5 h (f).

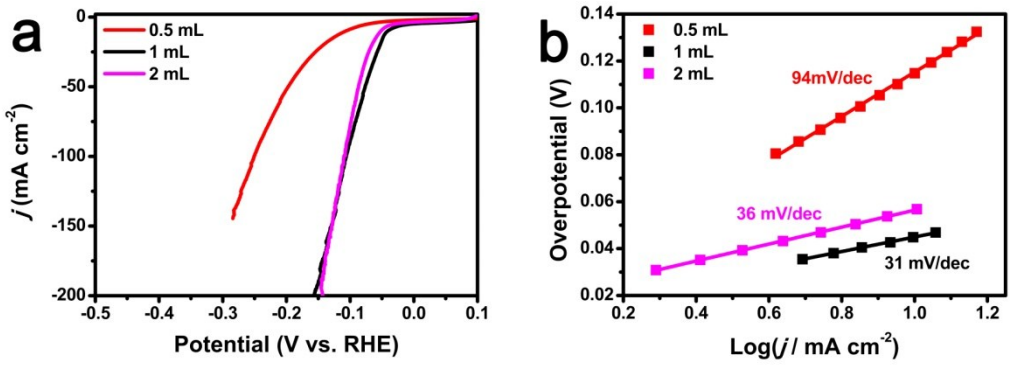

Figure S3. Polarization curves (a) and Tafel plots (b) of $NiMoO_{4-x}/MoO_2$ synthesized with different amount of H_2O_2 (1 M KOH, pH = 14).

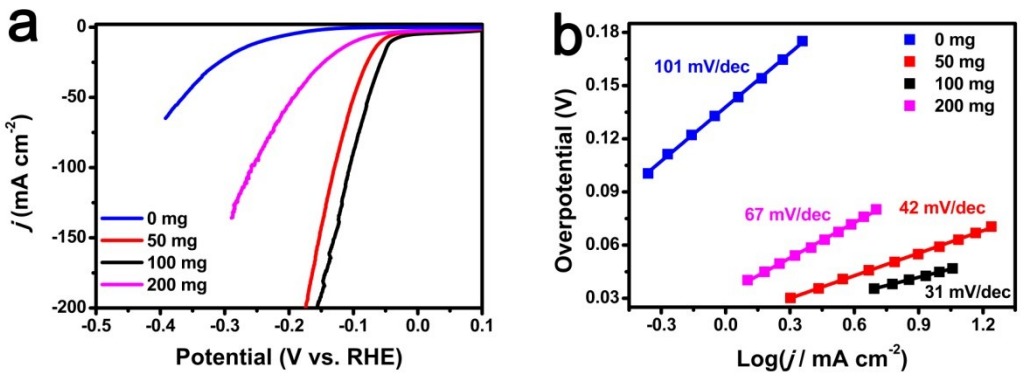

Figure S4. Polarization curves (a) and Tafel plots (b) of $NiMoO_{4-x}/MoO_2$ synthesized with different amount of molybdenum powder (1 M KOH, pH = 14).

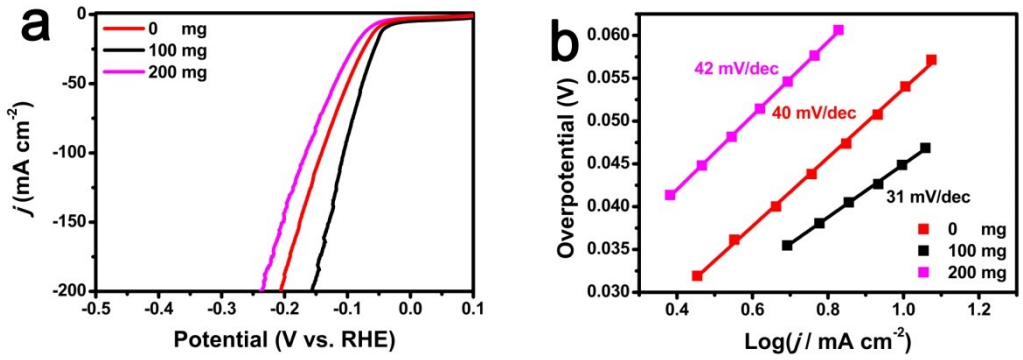

Figure S5. Polarization curves (a) and Tafel plots (b) of $NiMoO_{4-x}/MoO_2$ synthesized with different amount of SDS (1 M KOH, pH = 14).

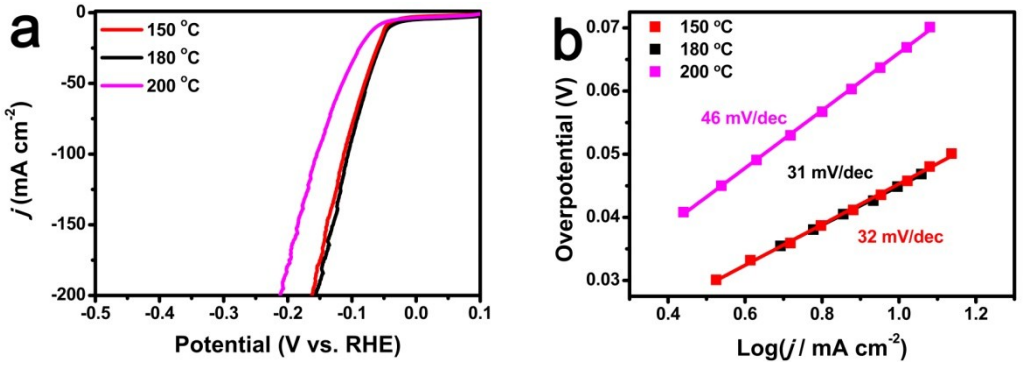

Figure S6. Polarization curves (a) and Tafel plots (b) of $NiMoO_{4-x}/MoO_2$ synthesized at different hydrothermal reaction temperature (1 M KOH, pH = 14).

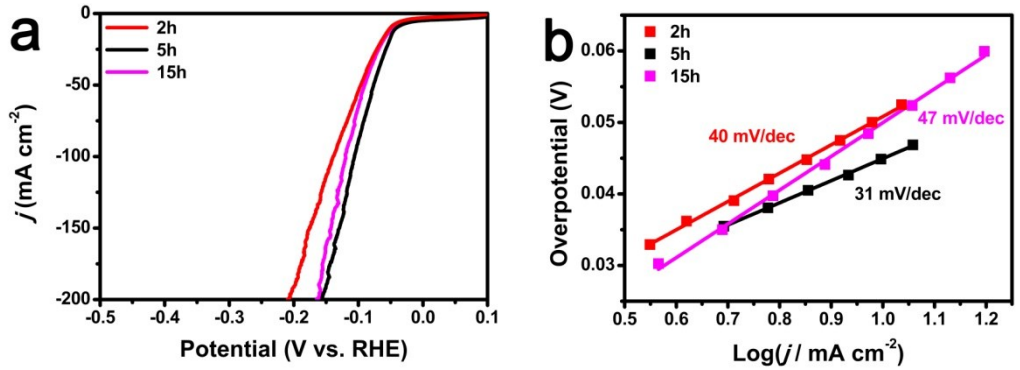

Figure S7. Polarization curves (a) and Tafel plots (b) of $NiMoO_{4-x}/MoO_2$ synthesized with different hydrothermal reaction time (1 M KOH, pH = 14).

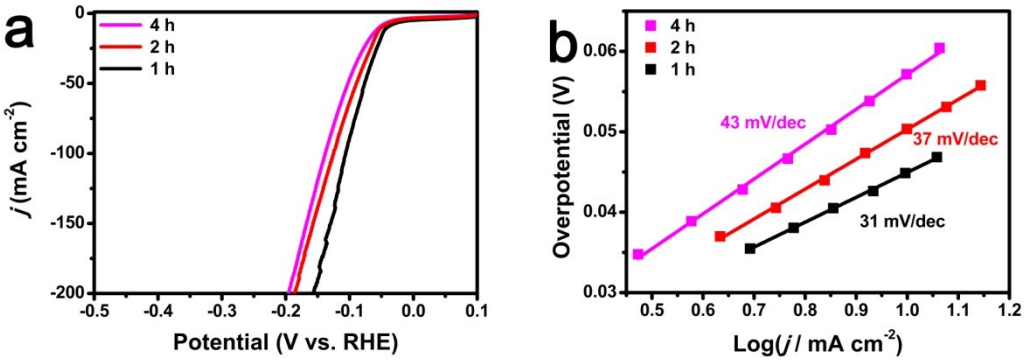

Figure S8. Polarization curves (a) and Tafel plots (b) of $NiMoO_{4-x}/MoO_2$ synthesized with different annealing time (1 M KOH, pH = 14).

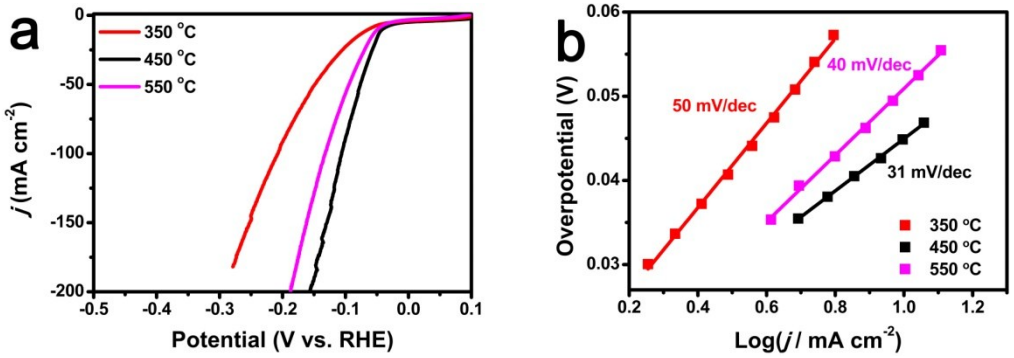

Figure S9. Polarization curves (a) and Tafel plots (b) of $NiMoO_{4-x}/MoO_2$ synthesized with different annealing temperature (1 M KOH, pH = 14).

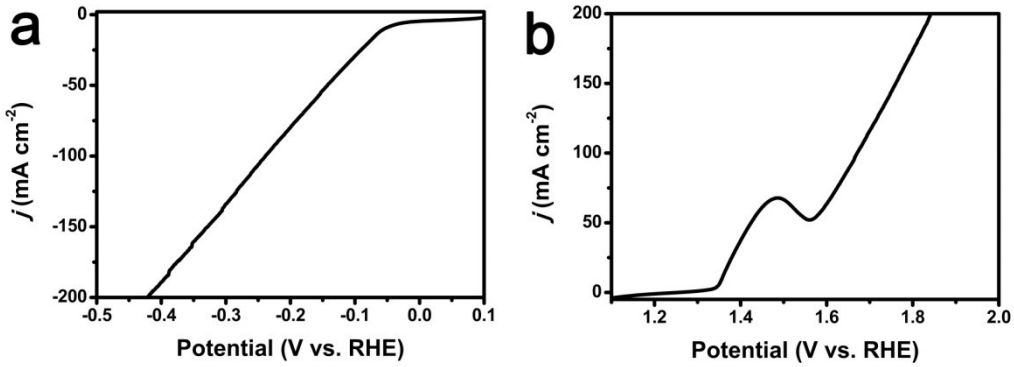

Figure S10. Polarization curves of $NiMoO_{4-x}/MoO_2$ for HER (a) and OER (b) without iR correction.

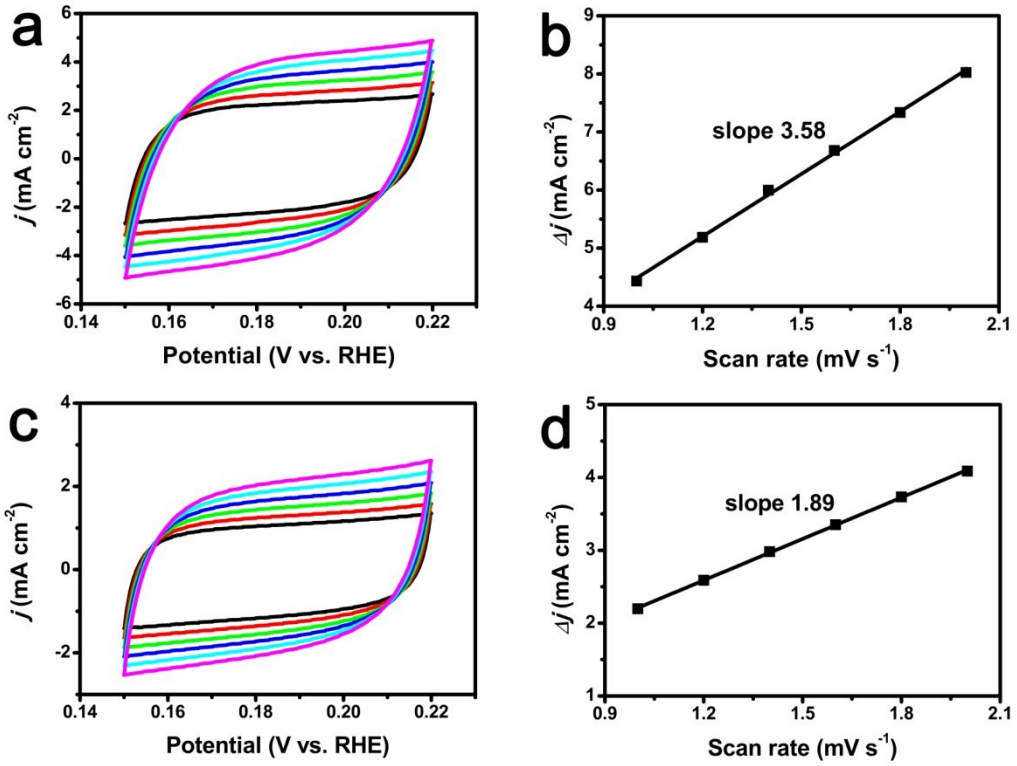

Figure S11. Electrochemical cyclic voltammogram of $NiMoO_{4-x}/MoO_2$ (a) and $NiMoO_4/MoO_2$ (c). Differences in current density ($\Delta j = j_a - j_c$) at 0.185 V vs RHE plotted against scan rates of $NiMoO_{4-x}/MoO_2$ (b) and $NiMoO_4/MoO_2$ (d) (the linear slope equivalent to twice of the double−layer capacitance C_{dl})

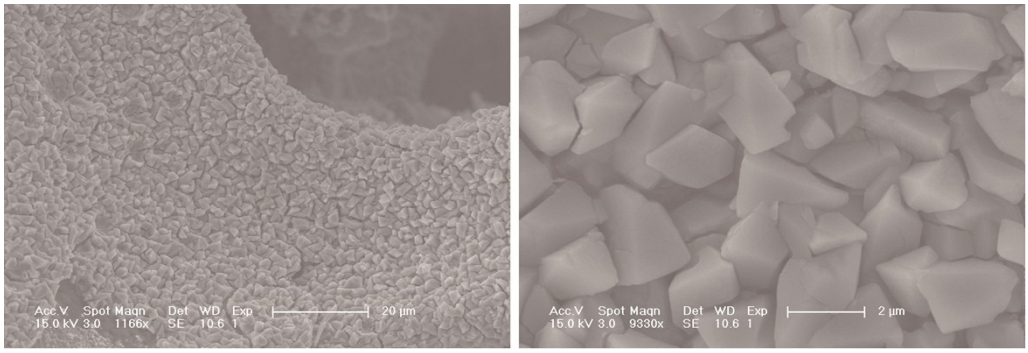

Figure S12. SEM images of $NiMoO_{4-x}/MoO_2$ with different magnification after HER test.

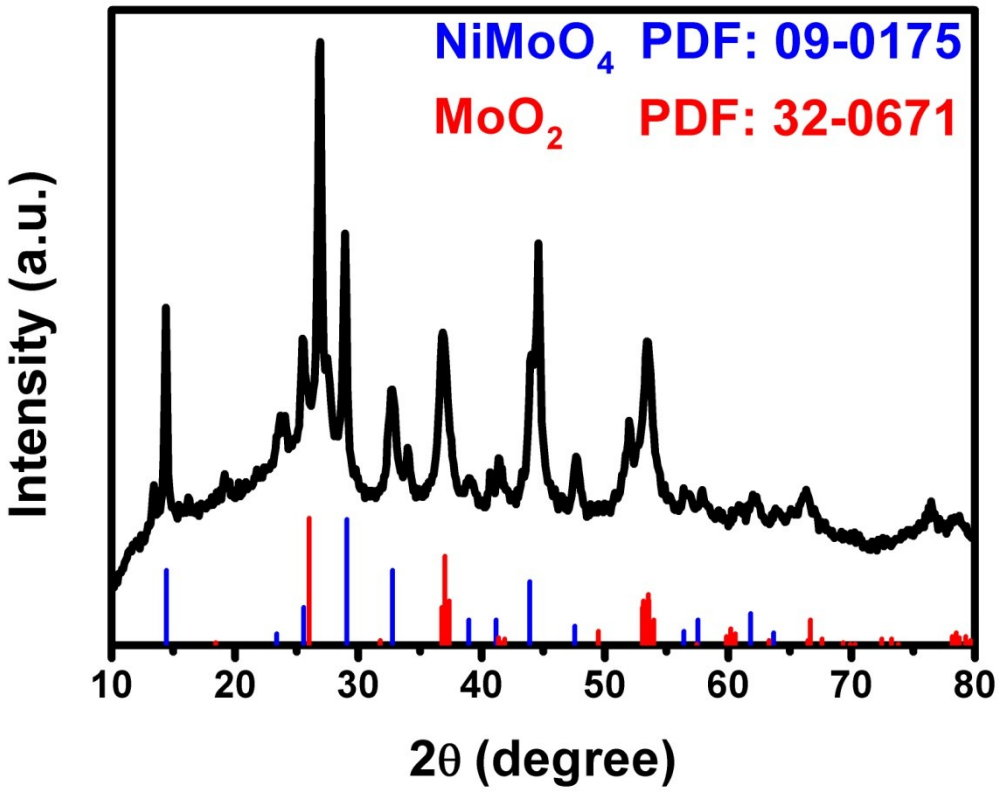

Figure S13. XRD pattern of $NiMoO_{4-x}/MoO_2$ after HER test.

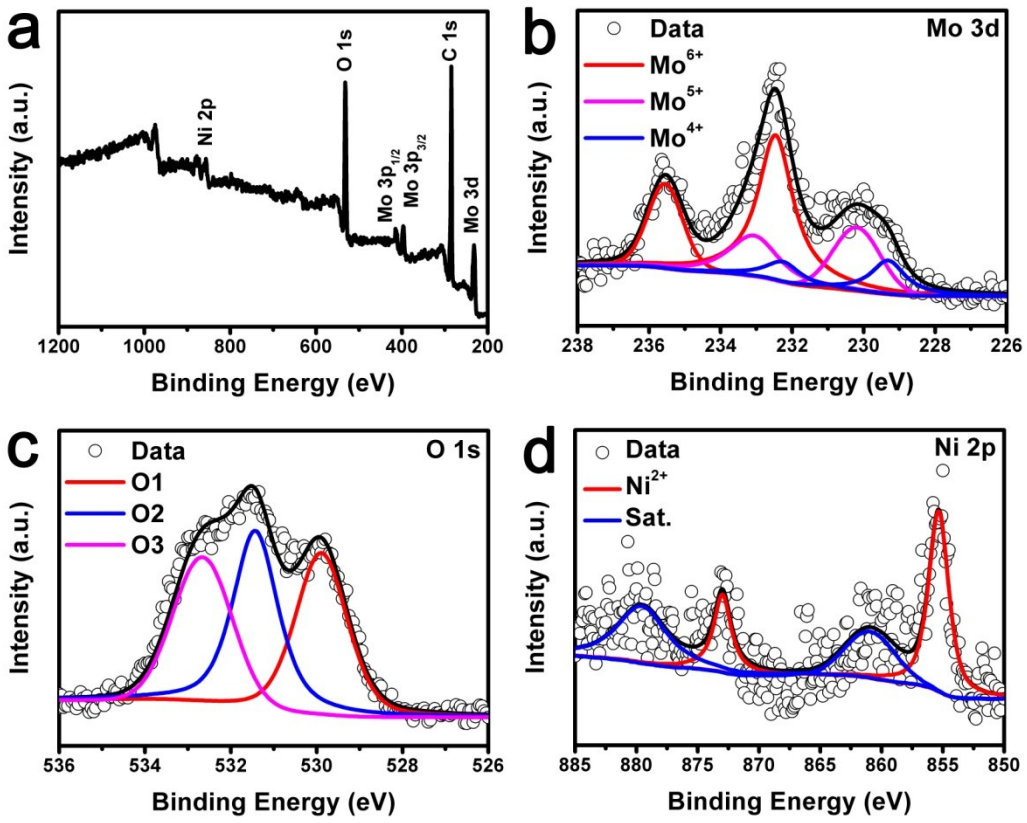

Figure S14. XPS survey spectrum (a) and high-resolution XPS spectra of Mo 3d (b), O 1s (c), and Ni 2p (d) of $NiMoO_{4-x}/MoO_2$ after HER test.

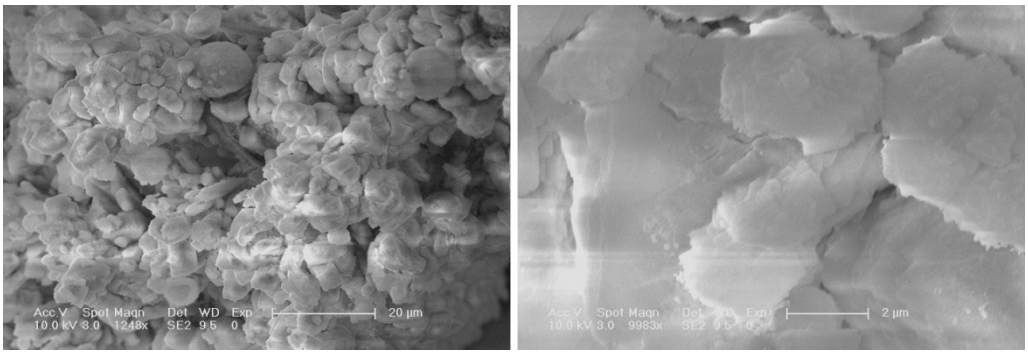

Figure S15. SEM images of $NiMoO_{4-x}/MoO_2$ with different magnification after OER test.

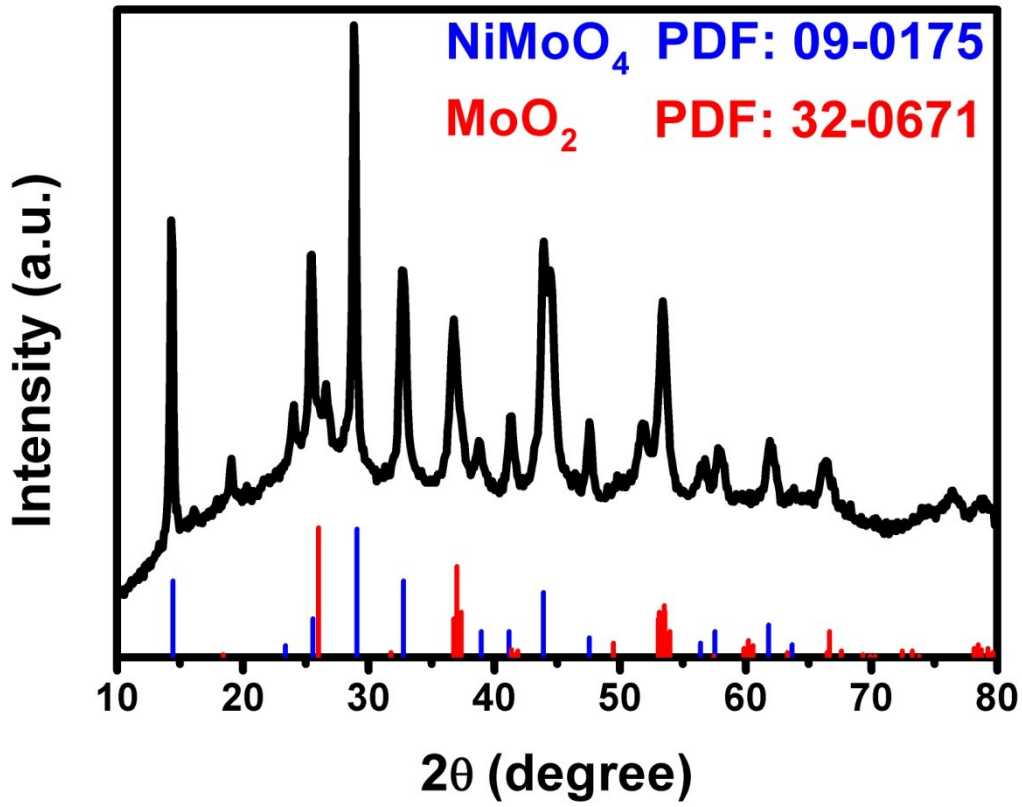

Figure S16. XRD pattern of $NiMoO_{4-x}/MoO_2$ after OER test.

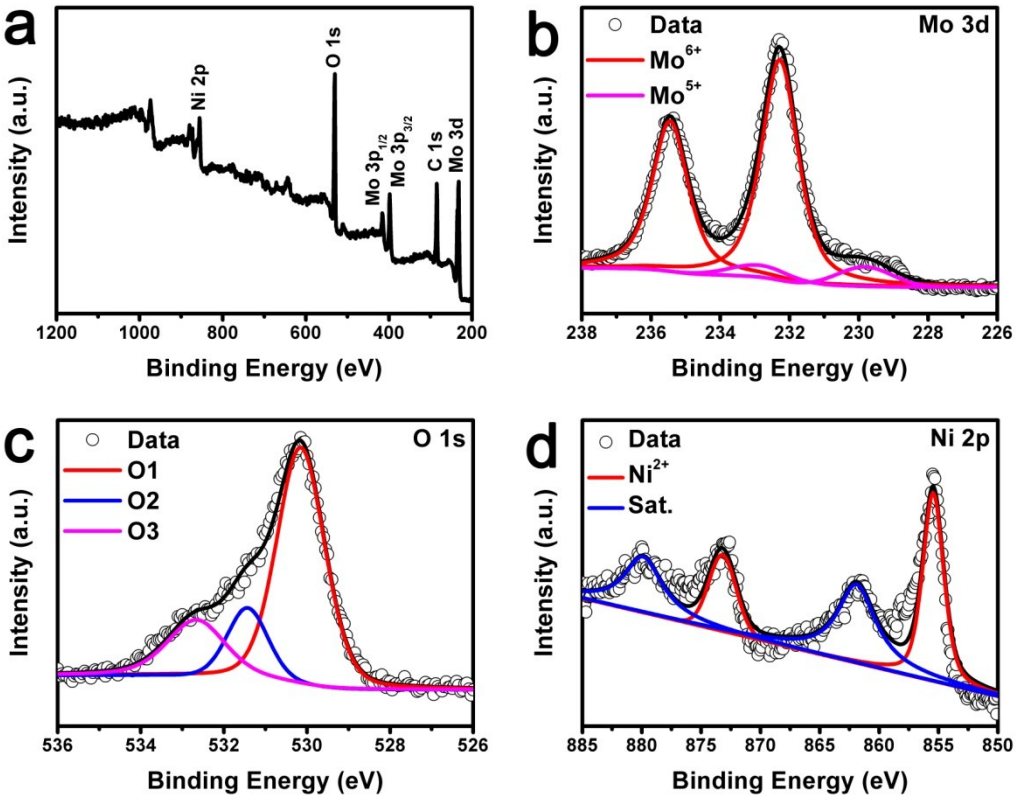

Figure S17. XPS survey spectrum (a) and high-resolution XPS spectra of Mo 3d (b), O 1s (c), and Ni 2p (d) of $NiMoO_{4-x}/MoO_2$ after OER test.

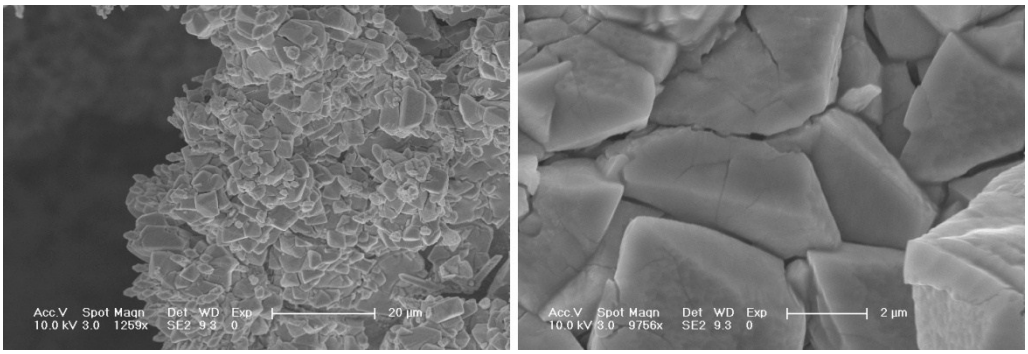

Figure S18. SEM images of $NiMoO_{4-x}/MoO_2$(air) with different magnification.

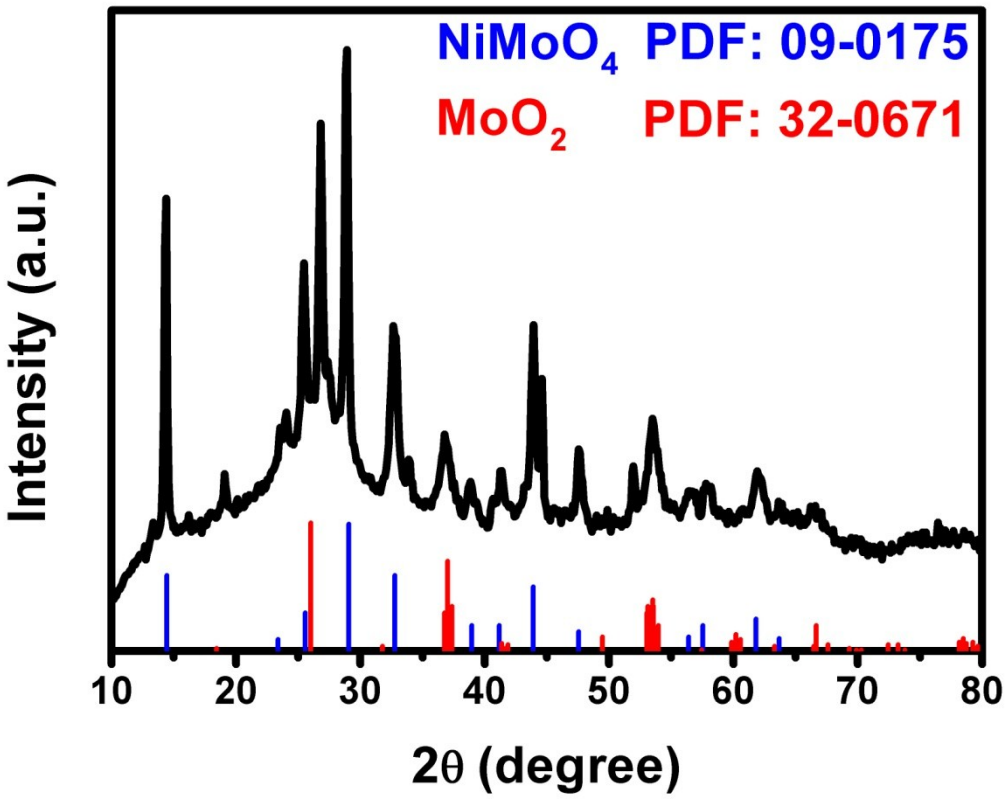

Figure S19. XRD pattern of $NiMoO_{4-x}/MoO_2$(air).

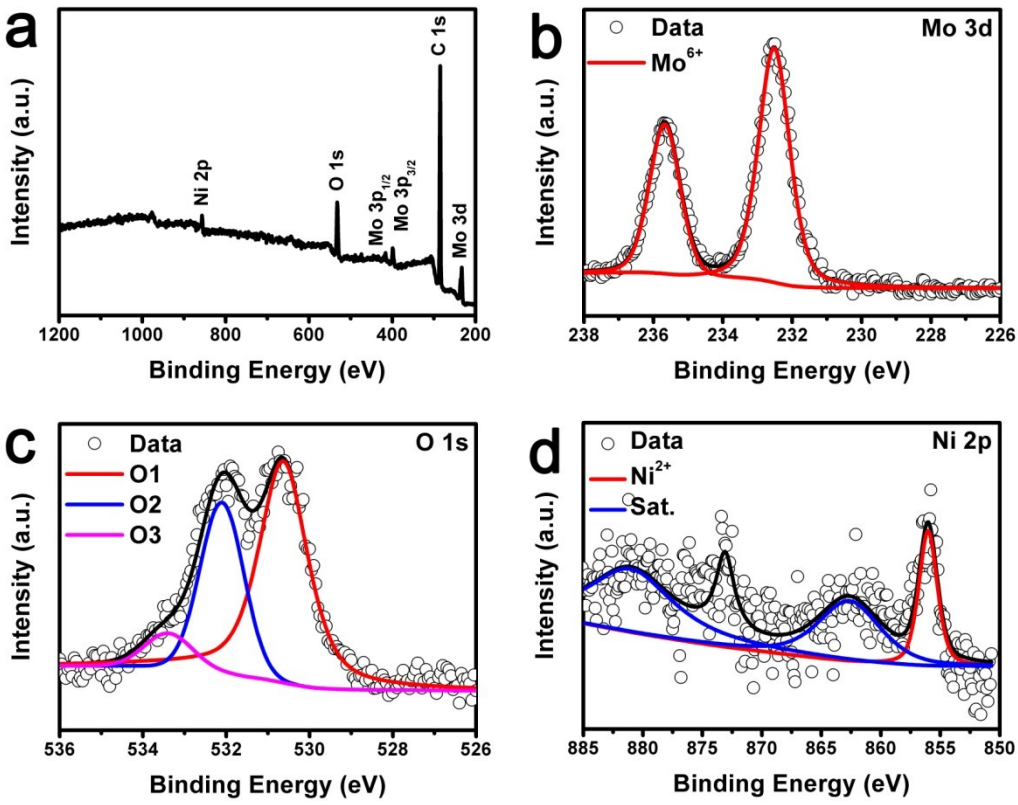

Figure S20. XPS survey spectrum (a) and high-resolution XPS spectra of Mo 3d (b), O 1s (c), and Ni 2p (d) of $NiMoO_{4-x}/MoO_2$(air).

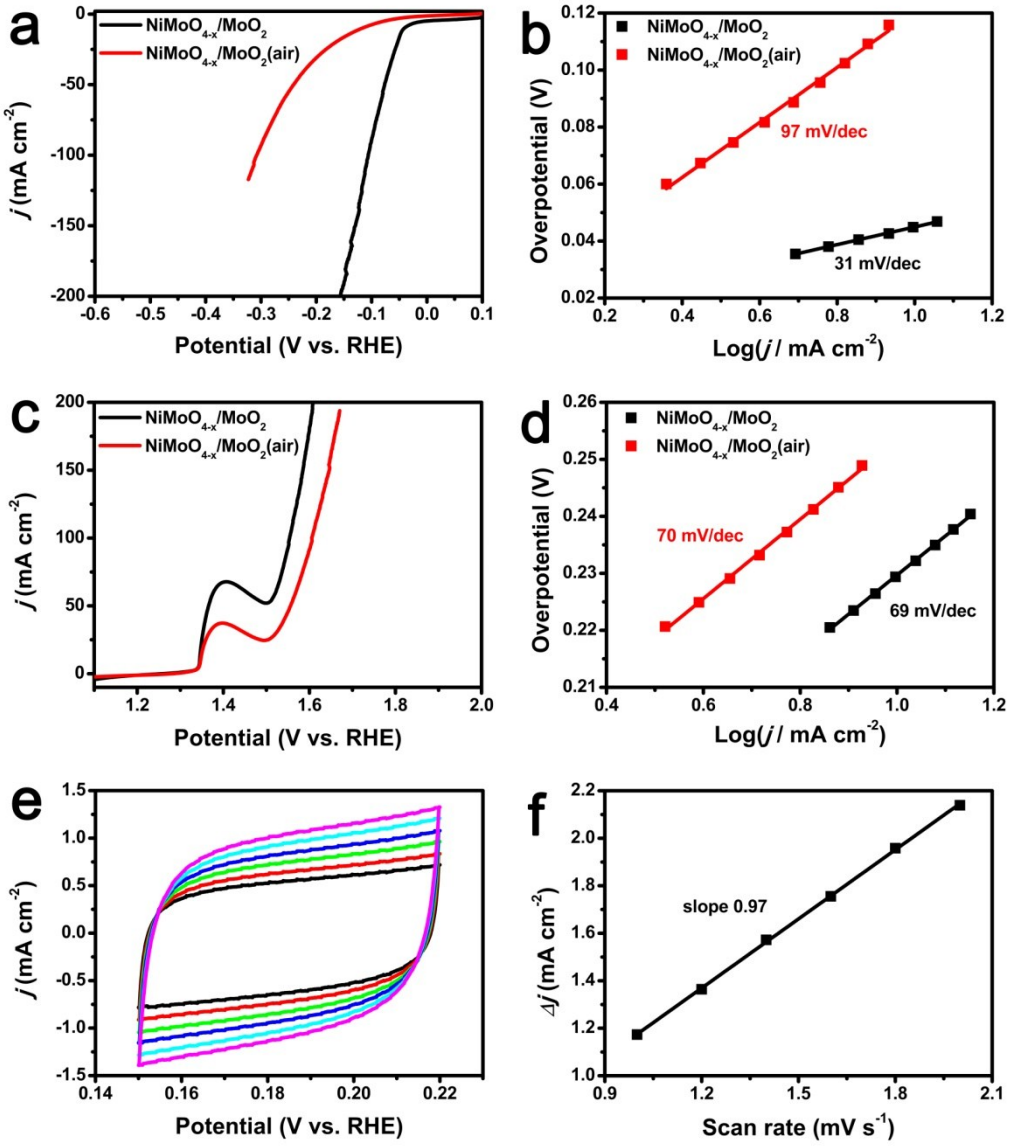

Figure S21. Polarization curves (a, c) and Tafel plots (b, d) of $NiMoO_{4-x}/MoO_2$ and $NiMoO_{4-x}/MoO_2$(air). Electrochemical cyclic voltammogram (e) and differences in current density ($\Delta j = j_a - j_c$) at 0.185 V vs RHE plotted against scan rates (f) of $NiMoO_{4-x}/MoO_2$(air).

Table S1 Comparison of HER and OER performance for $NiMoO_{4-x}/MoO_2$ with other electrocatalysts.

Catalyst	Current density (j, mA/cm^2)	η at the corresponding j for HER (mV)	η at the corresponding j for OER (mV)	Ref.
$NiMoO_{4-x}/MoO_2$	10	41	233	This work
Porous MoO_2 Nanosheets	10	27	260	*Adv. Mater.* 2016, **28**, 3785
Mesoporous MoO_{3-x}	10	140	--	*Adv. Energy Mater.*, 2016, 1600528.
$MoNi_4$	10	15	--	*Nature Commun.*, 2017, **8**, 15437.
$MoNi_4/MoO_{3-x}$ Nanorod	10	17	--	*J. Am. Chem. Soc.* 2011, **137**, 14023
Porous MoC_x	10	142	--	*Nature Commun.*, 2015, **6**, 6512.
Porous NiMoN	10	108	--	*Adv. Energy Mater.*, 2016, 1600221.
Hollow $NiMo_3S_4$	10	257	--	*Angew. Chem. Int. Ed.*, 2016, **55**,15240
MoS_2/RGO	10	150	--	*J. Am. Chem. Soc.* 2011, **133**, 7296
defect-rich MoS_2	13	200	--	*Adv. Mater.* 2013, **25**, 5807
$NiMoN_x/C$	2	170	0.24	*Angew. Chem. Int. Ed.* 2012, **51**, 6131
Co_9S_8@MoS_2/CNFs	10	190	430	*Adv. Mater.* 2015, **27**, 4752
Amorphous $CoMoS_4$	10	143	342	*Nanoscale*, 2016, **8**, 18887
$Co_{0.6}Mo_{1.4}N_2$	10	200	--	*J. Am. Chem. Soc.* 2013, **135**, 19186
MoB_2	10	120	--	*J. Am. Chem. Soc.* 2017, **139**, 12370
Ni-Mo	10	65	--	*ACS Nano*, 2016, **10**, *10397*